Astron. Astrophys. 275, 283–292 (1993)

ASTRONOMY AND ASTROPHYSICS

Uncombed fields as the source of the broad-band circular polarization of sunspots

S.K. Solanki and C.A.P. Montavon

Institute of Astronomy, ETH-Zentrum, CH-8092 Zürich, Switzerland

Received December 3, 1992; accepted April 3, 1993

Abstract. We investigate the production of broad-band circular polarization (BBC) of sunspots using a model inspired by the discovery of small-scale variations of magnetic inclination in sunspot penumbrae. The proposed model is a simple representation of a horizontal magnetic flux tube embedded in an inclined magnetic field, with a flow in either one or both components (Evershed flow). This model is shown to produce a sizeable BBC without requiring substantial net vertical gradients of the magnetic vector. It reproduces the BBC observations in a qualitatively correct and quantitatively acceptable manner for reasonable values of its free parameters. In addition, our model also explains the crossover effect observed in sunspot penumbrae. The fits to the observations support the presence of a larger velocity in the horizontal magnetic filaments than in the inclined field. We point out that the BBC is complementary to high resolution images in that it diagnoses the height variation of the small-scale structure of sunspot magnetic fields. By combining the results from both techniques we outline the 3-D fine-scale structure of the magnetic field in the photospheric layers of sunspot penumbrae. The most important result is that the two differently inclined components of the field do not simply form vertical sheets, but rather must have a horizontal interface near the level of line formation.

Key words: Sun: sunspots – Sun: magnetic fields

1. Introduction

Broad-band circular polarization (BBC) in sunspots was first detected by Illing et al. (1974a,b, 1975) and later observed by Kemp & Henson (1983), Henson & Kemp (1984), Makita (1986) and Makita & Ohki (1986). From these observations, particularly the extensive investigation of Makita & Ohki (1986), Sánchez Almeida & Lites (1992) distilled the following three empirical rules:

1. The broad-band circular polarization is largest in the limb-side penumbra close to the apparent magnetic neutral line, where the amplitude of the Stokes V profile is smallest.
2. The centre-side penumbra exhibits a smaller BBC of opposite sign to the BBC of the limb-side penumbra.
3. The sign of the blue lobe of the Stokes V profile in the umbra or centre-side penumbra corresponds to the sign of the maximum BBC in the limb-side penumbra.

Rules 2 and 3 are consistent with the area asymmetry of Stokes V profiles of 1.56 μm lines in sunspots near the solar limb (Solanki et al. 1993b). To these three empirical rules we add a fourth:

4. The maximum BBC of both the centre-side and limb-side penumbrae shows a distinct centre-to-limb variation (CLV). The BBC of both reaches a global maximum between $\mu = \cos\theta = 0.7$ and 0.8 (θ is the heliocentric angle).

The BBC of sunspots must still be considered unexplained. A number of attempts have been made to explain the observations, with increasing degrees of success, but no model exists which explains the BBC without violating some other basic observation of sunspots. The shortcomings of earlier models by Illing et al. (1975), Skumanich & Lites (1987), Auer & Heasley (1978), Landmann & Finn (1979) and Makita (1981, 1986) have been compellingly discussed by Sánchez Almeida & Lites (1992), and we shall not repeat their arguments. In addition to the investigations mentioned above, Illing (1981) proposed molecular lines, whose V profiles are very asymmetric even in the absence of velocity gradients, as a possible source of the BBC, but Makita (1986) demonstrated that it is definitely atomic lines which are responsible for the bulk of the BBC. He thus also ruled out continuum polarization as a source of the BBC in the visible part of the spectrum, although it may contribute to the measured signal in the infrared (Kemp & Henson 1983).

Finally, Sánchez Almeida & Lites (1992) introduced a model based on a smooth longitudinal gradient in the magnetic inclination, γ, to the line-of-sight (LOS). Like Makita, they qualitatively reproduce empirical rules 1–3 of the BBC, but even a change in γ of 40°–60° within the photospheric layers of the penumbra produces a BBC that is still three times smaller than the observed values. Now, 40–60° is a very significant change in inclination over a height range of only 400–600 km and should produce considerable electric currents, as already

Send offprint requests to: S.K. Solanki

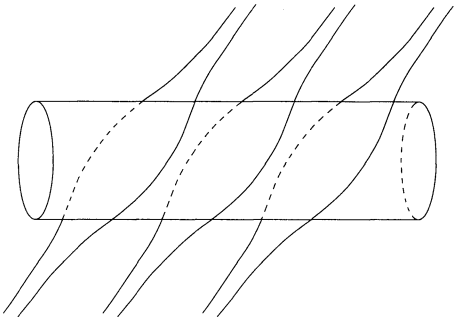

Fig. 1. Sketch of the proposed fine-scale structure of the magnetic field in sunspot penumbrae. The field is composed of two components, a flux-tube component, represented by the horizontal cylinder, and a more inclined magnetic field, indicated by the field lines crossing the flux tube at an angle

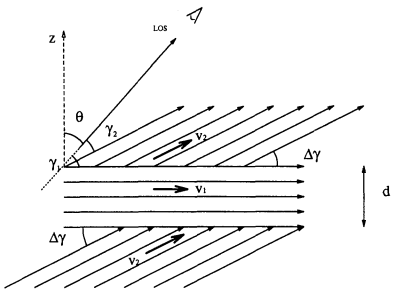

Fig. 2. Sketch of the magnetic and velocity structure of the 3-layered model, which schematically represents a vertical cut along the axis of the horizontal flux tube. Indicated are the vertical direction in the atmosphere (z), the direction to the observer (LOS), the angle between z and the LOS (θ), the angles between the LOS and the magnetic vectors of the horizontal and inclined magnetic components (γ_1 and γ_2, respectively), the angle between the magnetic vectors of the two components ($\Delta\gamma$), the velocities in the horizontal and inclined components (v_1 and v_2, respectively), and d, the diameter of the horizontal flux tube

noted by Sánchez Almeida & Lites (1992). In particular, it is over an order of magnitude larger than the limit on $\mathrm{d}\gamma/\mathrm{d}z$ set by Solanki et al. (1993a). A large-scale $\mathrm{d}\gamma/\mathrm{d}z$ of the magnitude proposed by Sánchez Almeida & Lites would cause horizontal static force balance in the sunspot to break down completely.

In the present paper we also model the BBC using cospatial longitudinal gradients of γ and of the LOS component of the velocity, v_{LOS}, but consider a 2-component penumbra with differently inclined fields in the 2 components, as suggested by the high-resolution observations of Beckers & Schröter (1969), Degenhardt & Wiehr (1991), Title et al. (1992), Schmidt et al. (1992), Lites et al. (1993) and Deubner et al. (1993). They find that the magnetic field of neighbouring penumbral filaments has inclinations which can differ by as much as 40°, giving the impression that the penumbral magnetic field is 'uncombed'. In order to produce a BBC, however, the two components cannot simply be horizontally separated from each other (as deduced from the high-resolution observations), but must also partly be vertically separated, i.e. magnetic field with one inclination must overly differently inclined field in at least some of the filaments. Consider, for example, a penumbral magnetic structure roughly of the form outlined by Parker (1992), i.e. nearly horizontal field lines emerging from the outer umbra or inner penumbra, embedded in an inclined penumbral field. Further, let the horizontal magnetic component be confined to discrete flux tubes, so that the inclined field lines curve around these tubes, much as a laminarly flowing fluid winds its way around a roughly cylindrical obstacle. Such a flux tube and surrounding field lines are illustrated in Fig. 1. This picture of penumbral fine structures is similar to that proposed by Wentzel (1992, see his Fig. 2). In his model the horizontal flux tube originates from inclined field which becomes unstable due to an upwelling in its footpoint, leading it to its fall (fallen flux tube).

For the proposed model, a vertical cut passing through the centre of the sunspot may in the penumbra be schematically represented by a simple 3-layered atmosphere, with a layer of nearly horizontal field sandwiched between layers of inclined field. This simplified model basically corresponds to considering only the central plane passing vertically through the horizontal flux tube, which greatly reduces the amount of radiative transfer calculations required to obtain the synthetic BBC signal. The geometry of the field in this model is outlined in Fig. 2. We have neglected changes in the azimuth χ at the interface between the two magnetic components, as are bound to be present in reality. A longitudinal gradient in χ also produces a net circular polarization (Makita 1986), but since the inclined field lines flowing around a horizontal flux tube (Fig. 1) give rise to χ gradients of opposite sign over the two horizontal halves of the flux tube, we expect the net contribution of such small-scale changes in χ to be small (cf. Makita 1986, who showed that switching the sign of the χ gradient changes the sign of the net circular polarization). In our model the inclination angle, γ, at the top of the atmosphere equals γ at the bottom. Nevertheless, strong γ gradients are present at the boundaries between the layers of different inclination. In the next section we show that the BBC produced at both the upper and the lower boundary has the same sign if a field-aligned velocity is introduced. Consequently, a net BBC is produced by the model, although no *net* $\mathrm{d}\gamma/\mathrm{d}z$ is present in it. In Sect. 3 we present series of test calculations which explore the BBC signature of the model and its dependence on various parameters. Section 4 contains a comparison between synthetic and observed BBC. In addition, we demonstrate there that the proposed model can also explain the cross-over effect. Finally, in Sect. 5 we discuss the results and draw conclusions.

2. Basic considerations

In the absence of significant continuum polarization, which is usually the case on the sun, an observable BBC is only produced if the total area of the positive lobes of the Stokes V profiles in the observed wavelength interval is not equal to the area of their negative lobes, i.e. if the integral over each V profile gives a net circular polarization (NCP). For normal, 2-lobed Stokes

V profiles the unsigned area of the blue lobe, A_b, must differ from the red lobe area, A_r, or equivalently,

$$\delta A = (A_b - A_r)/(A_b + A_r) \neq 0 \,. \tag{1}$$

For the mechanism based on longitudinal gradients of field strength, B, and line-of-sight component of the velocity, $v_{\rm LOS}$, proposed by Illing et al. (1975), which is mainly responsible for the δA seen in solar plages (Grossman Doerth et al. 1988, 1989; Solanki 1989; cf. Sánchez Almeida et al. 1988, 1989), Solanki & Pahlke (1988) pointed out that the sign of δA depends on the signs of the gradients of B and $v_{\rm LOS}$:

$$\mathrm{sign}(\delta A) = -\mathrm{sign}\left(\frac{\mathrm{d}v_{\rm LOS}}{\mathrm{d}\tau}\cdot\frac{\mathrm{d}|B|}{\mathrm{d}\tau}\right) \,, \tag{2}$$

where τ is the continuum optical depth and $v_{\rm LOS} > 0$ for a velocity directed away from the observer. Similarly, we can also predict the sign of the δA produced by gradients of γ and $v_{\rm LOS}$:

$$\mathrm{sign}(\delta A) = -\mathrm{sign}\left(\frac{\mathrm{d}v_{\rm LOS}}{\mathrm{d}\tau}\cdot\frac{\mathrm{d}|\cos\gamma|}{\mathrm{d}\tau}\right) \,. \tag{3}$$

The similarity between Eqs. (2) and (3) is remarkable. Note that Eq. (3) is only valid as long as $\cos\gamma$ does not change sign along a ray within the formation height range of a spectral line. Otherwise Stokes V can assume a complex shape with three or more lobes and the definition of δA (Eq. 1) breaks down.

Nevertheless, with the help of this relation, which we tested numerically, we can illustrate that the asymmetry produced by the upper and lower boundary of a horizontal flux tube embedded in an inclined (penumbral) field has the same sign. Consider the four simple cases shown in Fig. 3. The four subfigures schematically represent (a) the upper boundary of a horizontal flux tube in the limbward penumbra, (b) the upper boundary of such a flux tube in the centre-side penumbra and (c) and (d) the lower flux-tube boundary in the limbward and centre-side penumbra, respectively. In this illustrative model we assume that $v \neq 0$ only in the horizontal magnetic component, i.e. $v_1 \neq 0$ and $v_2 = 0$ (throughout the paper all quantities referring to the horizontal magnetic component are identified by subscript 1, those referring to the inclined magnetic component by subscript 2). It may be seen from Fig. 3 that for the illustrated cases $180° > \gamma_1 > \gamma_2 > 90°$, i.e. $|\cos\gamma_1| > |\cos\gamma_2|$, in the limbward penumbra, while $90° > \gamma_1 > \gamma_2 > 0°$, i.e. $|\cos\gamma_2| > |\cos\gamma_1|$, in the centre-side penumbra. Noting that τ increases away from the observer, so that $v_{\rm LOS} > 0$ is directed towards increasing τ, we find that $\mathrm{d}v_{\rm LOS}/\mathrm{d}\tau$ and $\mathrm{d}|\cos\gamma|/\mathrm{d}\tau$ in the four cases have the following signs,

$$\begin{aligned}
&(a)\quad \frac{\mathrm{d}v_{\rm LOS}}{\mathrm{d}\tau} > 0 \quad \text{and} \quad \frac{\mathrm{d}|\cos\gamma|}{\mathrm{d}\tau} > 0 \,,\\
&(b)\quad \frac{\mathrm{d}v_{\rm LOS}}{\mathrm{d}\tau} < 0 \quad \text{and} \quad \frac{\mathrm{d}|\cos\gamma|}{\mathrm{d}\tau} < 0 \,,\\
&(c)\quad \frac{\mathrm{d}v_{\rm LOS}}{\mathrm{d}\tau} < 0 \quad \text{and} \quad \frac{\mathrm{d}|\cos\gamma|}{\mathrm{d}\tau} < 0 \,,\\
&(d)\quad \frac{\mathrm{d}v_{\rm LOS}}{\mathrm{d}\tau} > 0 \quad \text{and} \quad \frac{\mathrm{d}|\cos\gamma|}{\mathrm{d}\tau} > 0 \,.
\end{aligned} \tag{4}$$

It then follows from Eq. (3) that $\delta A < 0$ in all four cases, i.e. the red lobe of Stokes V has a larger area than its blue lobe. Now, the NCP is given by $\int V\mathrm{d}\lambda / \int I_c\,\mathrm{d}\lambda$, so that the sign of the NCP produced at the upper and lower boundaries is the same. Consequently, a non-zero NCP is produced by the model, although γ, B and v above and below the horizontal flux tube are the same. Secondly, since δA is always negative and the sign of Stokes V changes from the centre-side to the limbward penumbra, the sign of the NCP also changes, in agreement with rule 2 (Sect. 1). Thirdly, since the sign of V in the umbra and the centre-side penumbra ($\gamma_1, \gamma_2 < 90°$) is opposite to the sign in the limbward penumbra ($\gamma_1, \gamma_2 > 90°$) and the red lobe of V is always stronger than its blue lobe, rule 3 also appears to be satisfied. Furthermore, one can easily show that for a sunspot of opposite polarity the NCP has the opposite sign (note that when the polarity is changed the magnetic arrows reverse direction, but the velocity arrows do not). Thus, even this simple qualitative illustration demonstrates the promise of the current model. Next we consider its implications more quantitatively.

We stress again that Eqs. (3) and (4) are only valid if either $0 \leq \gamma < 90°$, or $90° < \gamma \leq 180°$ at all heights (i.e. if the magnetic field always has the same polarity relative to the observer). An NCP is also produced if the magnetic polarity changes sign along the line-of-sight, but Eqs. (3) and (4) no longer provide an adequate description of this case.

3. Numerical test calculations

We have carried out two sets of test calculations. The first for two-layered models similar to those shown in Fig. 3, the second for the three-layered model described in Sect. 1. We consider the properties of the 2-layered model in some detail, since, due to the presence of a single interface, its results are easier to interpret and understand than those of the 3-layered model. Both models have in common that the boundary between two layers is sharp and that within each layer the magnetic and velocity fields are homogeneous. The thermal stratification in all layers corresponds to an interpolation between the quiet-sun and umbral models of Maltby et al. (1986), chosen such as to reproduce 1.56 μm line profiles observed in the penumbra (Solanki et al. 1993b). For numerical convenience we let the width of the boundary between two layers equal one step in the tabulated atmosphere, i.e., $\Delta \log\tau \approx 0.1$.

Following Sánchez Almeida & Lites (1992) we consider the $g = 2.5$, Fe I 6302.5 Å line, which is an often observed line in sunspots. Atomic data for the line were taken from Moore

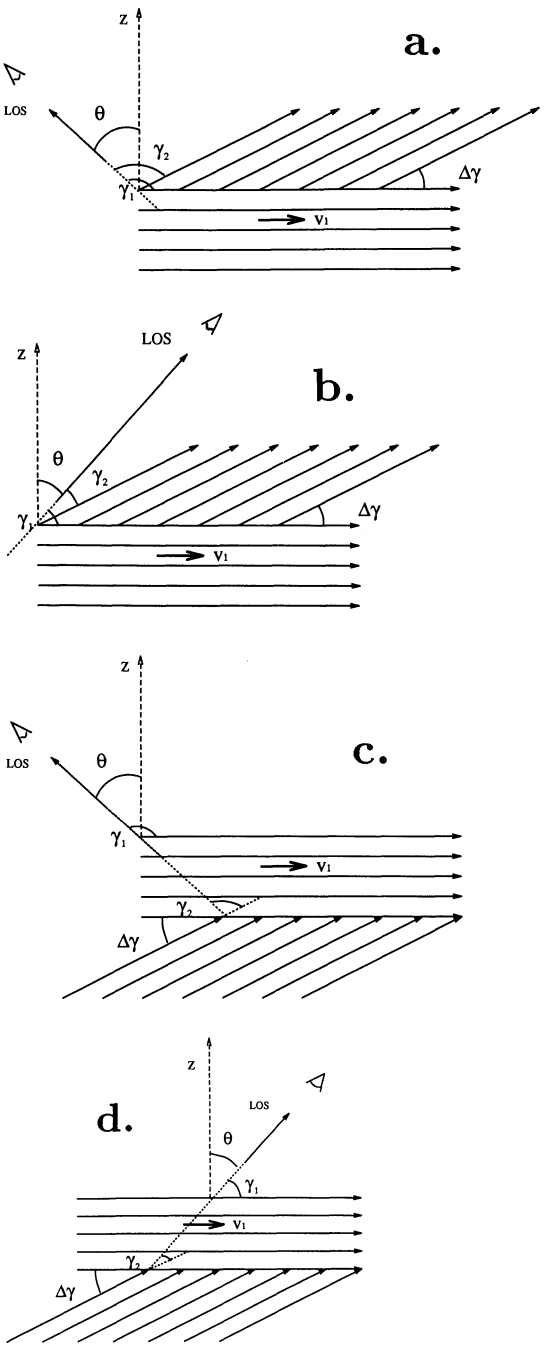

Fig. 3a–d. Schematic representation of the magnetic geometry at the upper (**a** and **b**) and lower (**c** and **d**) boundary of the central plane of a horizontal flux tube containing a flow. The tube is embedded in an inclined magnetic field. z, $\cos\theta$, γ_1, γ_2 and $\Delta\gamma$ are indicated (see Fig. 2)

(1972) and Thévenin (1990), and the radiative transfer was carried out using a code incorporating routines written by Murphy (1990), that are based on the DELO technique (Rees et al. 1989). Using this line not only has the advantage that our calculations can be compared to those of Sánchez Almeida & Lites (1992), but also that, being a medium-strong line, λ 6302.5 Å is representative of the lines most important for the production of BBC (stronger lines give a greater NCP, but are rarer). For example, in the spectral window of Makita & Ohki (1986), 5250 ± 7.5 Å, a consultation of a solar spectral atlas suggests that there is roughly one line of similar or slightly greater strength per Å of spectrum (and hardly any that are much stronger). Therefore, integrating the synthetic V profiles over a 1 Å interval gives an NCP which may be considered to be a conservative estimate of the BBC expected in the spectral window of Makita & Ohki (1986). Consequently, when comparing the model calculations with the observations, we identify this NCP with the BBC.

3.1. Two-layered model

The two-layered model used for numerical calculations differs from the one illustrated in Fig. 3 by the fact that we allow both layers to have a velocity and also let the field strength be different in the two layers. The results discussed in the present section refer in general to a model in which the horizontal component underlies the vertical component, but the results for the opposite geometry are similar. We test the influence of different parameters by 'observing' the model at different angles $\gamma = (\gamma_1 + \gamma_2)/2$ for a sunspot of positive polarity. We usually vary γ between 0 and 180°, which roughly corresponds to following a sunspot from one solar limb to the other. Although the variation of γ is coupled to a variation of θ, we find that if we vary only θ, while leaving γ fixed, then we obtain a practically negligible change in NCP (Montavon 1992), so that the θ variation can be neglected, in agreement with Makita (1986). For simplicity and consistency we therefore keep the continuum τ level of the boundary between the two layers, τ_b, constant. In the following we describe the results of such calculations. We postpone a quantitative comparison with the observations until Sect. 4.

First, consider the dependence on τ_b. Unsurprisingly, the NCP is largest when the boundary between the layers lies at a height at which Fe I 6302.5 Å obtains a large contribution, namely at $-1 \gtrsim \log\tau_b \gtrsim -1.5$. A more detailed discussion of the influence of $\log\tau_b$ is given in Sect. 3.2. For the rest of Sect. 3.1 we use $\log\tau_b = -1.5$.

Next we consider the influence of the velocity amplitude. Figure 4 shows the NCP as a function of γ for different $v = v_1 = v_2$ (the velocity in both magnetic components is assumed to be the same). $B = B_1 = B_2 = 1500$ G and $\Delta\gamma = |\gamma_2 - \gamma_1| = 10°$ for all curves. Within the considered velocity range, which encompasses the typically observed, spatially averaged Evershed velocities, the NCP reacts practically linearly to v. Changing v_1 and v_2 by the same factor only changes the magnitude of the NCP, but not its dependence on γ. The maximum NCP is produced at $\gamma = 90°$. Note that in our model the LOS lies parallel to the boundary between the two magnetic layers when $\gamma_1 = 0$ or 180°, i.e. when we 'observe' along the axis of the horizontal flux-tube. At these γ_1 values the NCP drops to zero. This is indicated by the vertical line at $\gamma = 175°$ in Fig. 4.[1] Similarly, the NCP disappears at $\gamma = 0$ and 180°, since $\mathrm{d}|\cos\gamma|/\mathrm{d}\tau = 0$.

[1] This situation is also reached for $\gamma = -5°$.

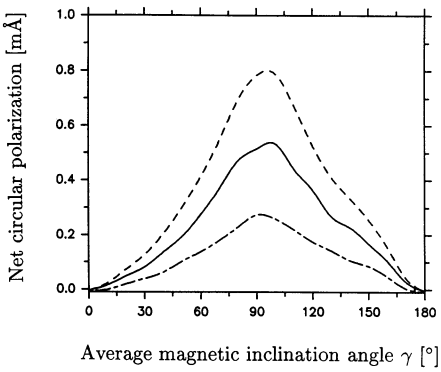

Fig. 4. Net circular polarization (NCP, see the text for its definition) vs. $\gamma = (\gamma_1 + \gamma_2)/2$, the angle between the LOS and the average magnetic field for a sunspot of positive polarity. Illustrated is the influence of the velocity magnitude. Dot-dashed curve: $v_1 = v_2 = 1\,\mathrm{km\ s^{-1}}$, solid curve: $v_1 = v_2 = 2\,\mathrm{km\ s^{-1}}$, dashed curve: $v_1 = v_2 = 3\,\mathrm{km\ s^{-1}}$, where v_1 is the velocity in the horizontal and v_2 in the inclined magnetic component. $\Delta\gamma = 10°$ and field strength $B = 1500$ G for all three curves

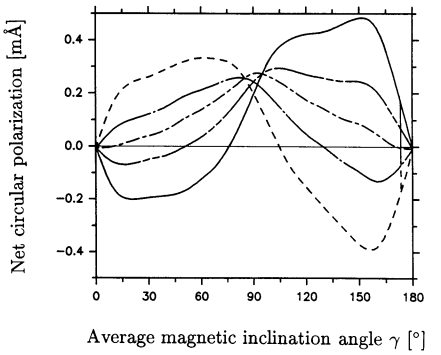

Fig. 5. NCP vs γ for different v_2/v_1 ratios. The v_2/v_1 values of the different curves are, from top to bottom in the left half of the diagram, 2, 1.25, 1, 0.8 and 0.5. Note that $v_1 + v_2$ is not the same for all curves. From top to bottom in the left half of the diagram: $v_1 = 0.5, 0.8, 1, 1, 1$ km s^{-1} and $v_2 = 1, 1, 1, 0.8, 0.5$ km s^{-1}, respectively. $\Delta\gamma = 10°$, $B = 1500$ G

As illustrated in Fig. 5, the v_1/v_2 ratio influences the shape of the NCP curves significantly. A $v_1 \neq v_2$ shifts the NCP peak to γ values closer to 0 or 180°. In addition, the NCP becomes negative at some angles. This is important, since without such a change of sign it is impossible to produce an NCP in the centre-side penumbra which is of opposite sign to the NCP produced in the limbward penumbra. The γ at which the sign of the NCP changes, γ_0, is given by

$$v_2 \cos(\gamma_0 - \Delta\gamma/2) = v_1 \cos(\gamma_0 + \Delta\gamma/2). \quad (5)$$

At γ_0 the LOS components of v_1 and v_2 are equal, so that $\mathrm{d}v_{\mathrm{LOS}}/\mathrm{d}\tau = 0$ and accordingly $\delta A = 0$.

The magnitude of the maximum NCP also increases with increasing asymmetry between v_1 and v_2, since the maximum $\mathrm{d}v_{\mathrm{LOS}}/\mathrm{d}\tau$ also increases. This is not so clearly visible from

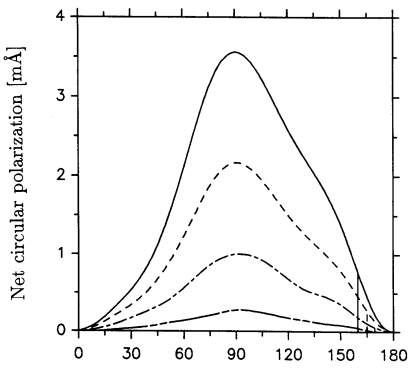

Fig. 6. NCP vs. γ for different $\Delta\gamma$. From top to bottom $\Delta\gamma = 40°$, 30°, 20° and 10°. $v_1 = v_2 = 1\,\mathrm{km\ s^{-1}}$, $B = 1500$ G

Fig. 5, since $v_1 + v_2$ is not the same for all curves. The linearity of the NCP's dependence on v_1 and v_2 continues to hold (within the range of tested values) in the sense that if, for example, the NCP curve obtained with $v_1 = 1\,\mathrm{km\ s^{-1}}$ and $v_2 = 2\,\mathrm{km\ s^{-1}}$ is added together with the curve for $v_1 = 2\,\mathrm{km\ s^{-1}}$ and $v_2 = 1\,\mathrm{km\ s^{-1}}$, then the result is identical with the curve obtained for $v_1 = v_2 = 3\,\mathrm{km\ s^{-1}}$!

Next, in Fig. 6, we show the NCP produced for $\Delta\gamma = 10, 20, 30$ and 40°, while keeping $v_1 = v_2 = 1\,\mathrm{km\ s^{-1}}$ and $B = 1500$ G fixed. Obviously, the NCP increases more strongly than linearly with $\Delta\gamma$. This is not surprising, since for most γ values an increase in $\Delta\gamma$ not only increases $\mathrm{d}|\cos\gamma|/\mathrm{d}\tau$, but also $\mathrm{d}v_{\mathrm{LOS}}/\mathrm{d}\tau$ if v_1 and v_2 are both non-zero.

Another parameter whose influence we have tested is the field strength B. We considered three cases, $B_1 = B_2 = B = 800$ G, 1500 G and 2000 G, which cover the range of B values found in the penumbra (e.g. Solanki et al. 1992). The parameter most strongly affected by B is the absolute value of the NCP, but even it changes by a factor of only 1.5 over the whole tested range of B values.

Finally, we test the influence of differences between the magnetic field strength in the two components on the BBC. In Fig. 7 we show the results for $B_1 = B_2 = 1500$ G (solid curve), $B_1 = 1500$ G, $B_2 = 1700$ G (dot-dashed curve) and $B_1 = 1700$ G, $B_2 = 1500$ G (dashed curve).[2] We chose the $\Delta B = |B_2 - B_1|$ values following Degenhardt & Wiehr (1991).

3.2. *Three-layered model*

In this section we present results of test calculations based on a 3-layered model representing a vertical cut along the axis of a horizontal flux tube embedded in an inclined field. This model has one additional free parameter compared to the 2-layered model, the diameter of the tube, d (see Fig. 2). We keep the τ level of the lower boundary of the horizontal flux tube fixed (irrespective of γ). However, since the flux tube has a fixed

[2] The gas pressure was not adjusted to take into account differences in the magnetic pressure.

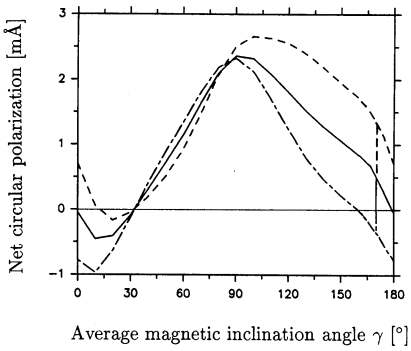

Fig. 7. NCP vs γ for different $B_1 - B_2$ values, where B_1 and B_2 are the field strengths in the horizontal and inclined magnetic components, respectively. Solid curve: $B_1 = B_2 = 1500$ G, dashed: $B_1 = 1700$ G and $B_2 = 1500$ G and dot-dashed curve: $B_1 = 1500$ G and $B_2 = 1700$ G. In all cases $v_2/v_1 = 0.8$ km s^{-1}, $\Delta\gamma = 20°$

geometrical width (in the vertical direction), its width on the τ scale varies substantially with γ. As in the 2-layered model, the NCP disappears for $\gamma_1 = 0$. We do not expect this artifact of the model to be visible in real observations, since even minute irregularities in inclination of the flux tube would lead to the production of an NCP at this γ value as well. In addition, for a horizontal flux tube, $\gamma_1 = 0$ is only reached right at the solar limb.

The dependence of the NCP produced by the 3-layered model on v_1, v_2, B_1, B_2, $\Delta\gamma$ and magnetic polarity is similar to that obtained with the 2-layered model (Sect. 3.1). Therefore, below we discuss only the parameters which are either not present or give substantially different results from the 2-component model.

The vertical diameter, d, of the flux tube also affects the NCP. It is largest for $d \approx 150$ km. For thicker tubes the BBC decreases slightly (if the lower boundary is kept fixed at $\log\tau = -1$), since the contribution of the upper boundary decreases as it lies at increasingly greater heights. For $d \ll 150$ km the flux tube becomes optically thin, so that it contributes less and less to the line, which then essentially sees only the layers of inclined field. Consequently, the NCP drops rapidly with decreasing d. For example, a flux tube with $d \approx 70$–80 km results in only half the NCP of a flux tube with $d = 150$ km.

Finally, we find that in the 3 layered model we obtain a sizeable NCP for a much larger range of heights of the lower boundary of the flux tube [$-2 \lesssim \log\tau_b(\text{lower}) \lesssim +1$ for $d \approx 150$ km] than for the 2-layered model, since both boundaries now contribute to the NCP. We also find that although the γ dependence of the NCP is a strong function of $\log\tau_b$ of the lower boundary, the averaged NCP produced by an ensemble of tubes distributed randomly in height has a very similar γ dependence to the NCP produced by a tube whose lower boundary lies at $\log\tau = -1.5$. Therefore, for the comparison with the observations in the next section we use NCP curves computed for flux tubes with their lower boundary at $\log\tau = -1.5$ and a diameter $d = 150$ km.

4. Comparison with observations

4.1. Broad-band circular polarization

The deliberations and calculations presented in Sects. 2 and 3 show that the proposed model, inspired by the recent detection of 'uncombed' magnetic fields in sunspot penumbrae and the $\Delta\gamma$ mechanism proposed by Sánchez Almeida & Lites (1992), satisfies the qualitative properties 1–3 (Sect. 1) of the observed BBC:

1. The BBC is largest near $\gamma \approx 90°$, i.e. close to the apparent neutral line, if v_1 and v_2 are not too different.
2. If $v_1 > v_2$, then for small γ ($0 \lesssim \gamma \lesssim 45°$), corresponding roughly to the centre-side penumbra of a sunspot observed near the limb, a small BBC of opposite sign to the BBC at $\gamma \gtrsim 90°$ is obtained.
3. The proposed model gives the correct sign and polarity rule of the BBC.

In addition, our model requires no strong *global* gradients of the magnetic vector to produce a BBC, so that it also satisfies the constraints on global magnetic gradients in the penumbra set by Solanki et al. (1993a). In the present section we compare the predictions of our model quantitatively with the measured BBC values.

We compare mainly with the CLV of the BBC of 41 sunspot groups observed by Makita & Ohki (1986). The CLV of the BBC of the sunspot observed by Illing et al. (1975) lies within the scatter of the observations of Makita & Ohki. Specifically we compare the model calculations with the maximum BBC values in the limbward and centre-side penumbrae as a function of θ (Fig. 3 of Makita & Ohki 1986). The maximum BBC has the advantage that it is a unique and objectively determinable quantity. Note, however, that due to smearing by the seeing, the maximum BBC of the observations is averaged over a considerable area in the penumbra.

When modelling the BBC we consider only fields with azimuths of 0° and 180°, i.e. we model a scan passing radially through the sunspot in a direction perpendicular to the limb. For a given θ value we calculate the NCP of Fe I 6302.5 Å, using the 3-layered model, at five radial positions in each (i.e. limb-side and centre-side) penumbra. These positions and the corresponding magnetic inclination angles relative to the vertical, γ', are indicated by the arrows in Fig. 8. The variation of γ' with r/r_p corresponds to an average over the published observational values compiled by Solanki & Schmidt (1993). As noted in Sect. 3, the calculated NCP corresponds roughly to the BBC expected for the wavelength interval observed by Makita & Ohki (1986).

For simplicity — the nature of this investigation is exploratory — we make a number of assumptions:

1. $\Delta\gamma$ is kept constant throughout the penumbra.
2. The atmosphere is assumed to be the same in all three layers.
3. v_1 and v_2 are taken to be independent of spatial position.
4. $B_1 = B_2 = B$ is independent of r/r_p.
5. The profiles are calculated along a single ray at each spatial position in the penumbra.

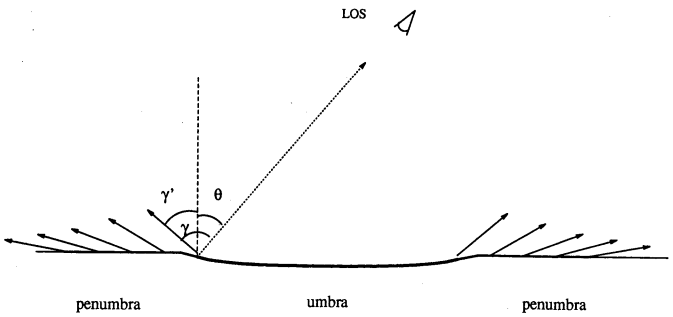

Fig. 8. Illustration of the positions in the sunspot and average magnetic inclinations γ' (angle between the vertical and the magnetic vector, averaged over both magnetic components), adopted when comparing with the observations

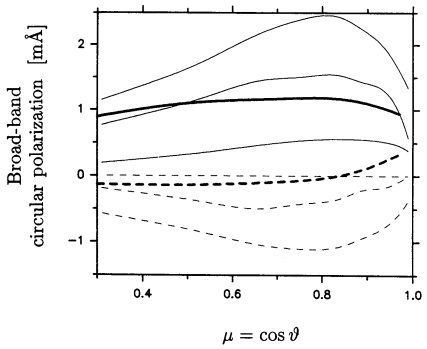

Fig. 9. Broad-band circular polarization (BBC) in the limb-side (solid) and centre-side (dashed) penumbra vs. $\mu = \cos\theta$. Thin curves represent observed BBC values, thick curves synthetic values produced by a 3-layered model with $v_1 = 2\,\mathrm{km\,s^{-1}}$ and $v_2 = 1.6\,\mathrm{km\,s^{-1}}$ (see text, Sect. 4.1, for details)

Assumptions 1–3, and partly 4, reflect the uncertainty in our empirical knowledge of many aspects of the fine-scale structure of sunspot magnetic fields. In order to take the limited spatial resolution of the observations into account, we average the BBC produced at all five radial positions in each penumbra. This may be too conservative, but we recall that by restricting ourselves to azimuths 0 and 180° in the model calculations, we have already selected the azimuths which we expect to give the largest BBC. Note that even if we do not spatially average at all, we still obtain similar results.

Observed and synthetic maximum BBC values are plotted vs. μ in Figs. 9 and 10. The thin curves represent the observations, the thick curves the results of the modelling. Solid curves refer to the limbward penumbra, dashed curves to the centre-side penumbra. For each penumbra we plot three observed curves. The middle curve is our estimate of the average of the measured maximum BBC values based upon Fig. 3 of Makita & Ohki (1986). The two outer curves are upper and lower envelopes to the data points and indicate the variation of the maximum BBC from one sunspot to the next. Figures 9 and 10 differ only in the curves due to the model. In Fig. 9 the underlying model parameters are $v_1 = 2\,\mathrm{km\,s^{-1}}$, $v_2 = 1.6\,\mathrm{km\,s^{-1}}$ (i.e. $v_2/v_1 = 0.8$), $\Delta\gamma = 20°$, $B = 1500$ G and $d = 150$ km, while in Fig. 10 they are $v_1 = 2\,\mathrm{km\,s^{-1}}$ and $v_2 = 1.2\,\mathrm{km\,s^{-1}}$ (i.e. $v_2/v_1 = 0.6$). The other parameters are the same as in Fig. 9.

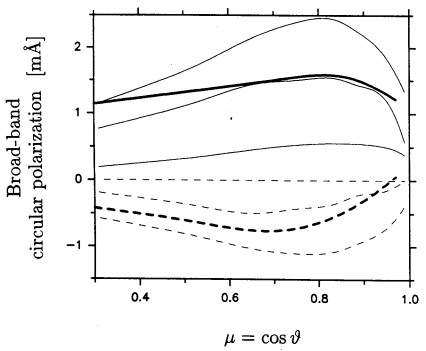

Fig. 10. Same as Fig. 9, but with synthetic curves produced by a model with $v_1 = 2\,\mathrm{km\,s^{-1}}$ and $v_2 = 1.2\,\mathrm{km\,s^{-1}}$

From a comparison between the two figures we note that the v_2/v_1 ratio affects the maximum BBC in three different ways:

a) The BBC becomes larger as v_2/v_1 decreases.
b) v_2/v_1 changes the ratio between the BBC of the limbward and the centre-side penumbra. The ratio approaches -1 for $v_2/v_1 \ll 1$.
c) The μ at which the BBC reaches its global maximum changes with v_2/v_1.

Obviously $v_2/v_1 = 0.6$ reproduces the observations better than $v_2/v_1 = 0.8$. The match to the data is quite reasonable, given the fact that we have only varied a single free parameter, v_2, in our simple model in order to fit the data (all other parameters have been kept fixed at values compatible with the observations or appearing otherwise reasonable, e.g., v_1, B, γ, T, $\Delta\gamma$).

Note that $v_2/v_1 \geq 1$ produces a BBC which differs qualitatively from the observations and can be ruled out. Thus, the measured BBC implies that the Evershed flow, although field-aligned, is on average more horizontal than the magnetic field, in agreement with direct measurements of the Evershed effect (e.g. Maltby 1964; Title et al. 1992). Given the large scatter in the measurements, the simplicity of the model and the uncertainties in free parameters such as B_1/B_2, we refrain from fine-tuning the model further in order to improve the fit.

There are claims in the literature that the Evershed flow is restricted to, or at least enhanced in, dark penumbral filaments (e.g. Abdussamatov & Krat 1970; Mamadazimov 1972; Stellmacher & Wiehr 1980; Title et al. 1992). This observation implies that only half or even less of the penumbral surface contributes to the spatially averaged BBC. The high efficiency of sharp interfaces in producing a BBC has the advantage that, for observationally consistent parameter values ($\Delta\gamma \approx 40°$, $v \approx 2$ $\mathrm{km\,s^{-1}}$), we can still easily reproduce the observed magnitude of the BBC if only the dark or only the bright filaments contribute.

Finally, we note that the wavelength dependence of the BBC measured by Kemp & Henson (1983) should be relatively straighforward to reproduce in general terms since it mainly reflects the density of lines (e.g. Mürset et al. 1988), except possibly in the infrared (see Kemp & Henson 1983). However, before modelling the BBC's wavelength dependence, a more thorough investigation of the NCP produced by spectral lines with widely different properties must be carried out, which is beyond the scope of the present paper.

4.2. Crossover effect

The crossover effect was first described by Babcock (1951) on Ap stars. In sunspots it has been observed or modelled by Grigorjev & Katz (1972, 1975), Golovko (1974), Mickey (1985a,b), Skumanich & Lites (1991) and Sánchez Almeida & Lites (1992). The observed V profiles typically have three (and sometimes more) lobes near the apparent neutral line in the penumbra and lose their usual, more-or-less antisymmetric, 2-lobed appearance, while Stokes I, Q and U appear relatively normal (Sánchez Almeida & Lites 1992). Golovko (1974) and Skumanich & Lites (1991) model the anomalous profile shapes using two magnetic components of opposite polarity. By introducing a velocity difference between the two components, it is possible to reproduce the observed profile shapes. Grigorjev & Katz (1975) and later Sánchez Almeida & Lites (1992) produced V profiles exhibiting the crossover effect using a single magnetic component and longitudinal gradients in $v_{\rm LOS}$ and χ, or $v_{\rm LOS}$ and γ.

As Fig. 11 shows, our model also produces atypical V profiles near $\gamma = 90°$. For the parameter values underlying the plotted profiles (3-layered model, $\Delta\gamma = 30°$, $v_1 = 2\,\mathrm{km\ s^{-1}}$, $v_2 = 1.2\,\mathrm{km\ s^{-1}}$, $B = 1200$ G), Fe I 6302.5 Å shows a maximum of three Stokes V lobes. Note that the V profiles for $\gamma \approx 90°$ are almost completely positive, with practically no negative lobe. This demonstrates the efficiency of the model in producing asymmetric V profiles and an NCP. For larger ratios of Zeeman splitting to non-magnetic line width, the line profile shape can be more complex with a greater number of peaks.

Therefore, the proposed model not only reproduces the observed BBC, but simultaneously also explains the crossover effect near the neutral line.

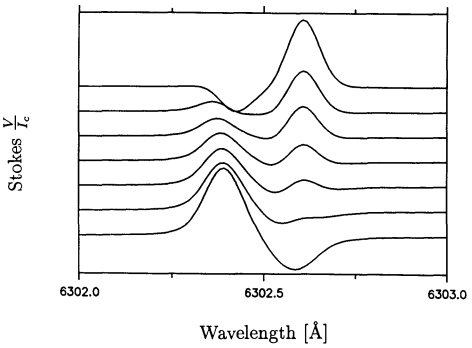

Fig. 11. Stackplot of synthetic Stokes V profiles of Fe I 6302.5 Å, produced by a 3-layered model with $v_1 = 2\,\mathrm{km\ s^{-1}}$, $v_2 = 1.2\,\mathrm{km\ s^{-1}}$, $B = 1200$ G, $\Delta\gamma = 30°$ and $d = 150$ km, near the apparent neutral line for $\theta = 60°$. The line profiles have been broadened by a macroturbulence of $2.5\,\mathrm{km\ s^{-1}}$. From top to bottom $\gamma = 100°, 95°, 92.5°, 90°, 87.5°, 85°$ and $80°$

5. Discussion and conclusions

In the present paper we have investigated the broad-band circular polarization produced by a simple model of the magnetic field in the penumbra. The model consists of layers with different magnetic inclinations containing field-aligned flows. It serves as a schematic representation of relatively horizontal tubes of magnetic flux embedded in an inclined penumbral field, based loosely on observations of 'uncombed' fields in sunspot penumbrae. It shares a number of features with the model of penumbral magnetic structure proposed by Wentzel (1992). The broad-band circular polarization is produced by the change in the magnetic inclination between two layers, $\Delta\gamma$, so that it relies mainly on the mechanism proposed by Sánchez Almeida & Lites (1992).

We show that if we assume values for the free parameters in the model that are supported by independent observations, then we not only reproduce the qualitative aspects of the observed BBC, but also obtain a reasonable quantitative fit to the observed CLV of the BBC, as well as a natural explanation of the crossover effect.

Consider now the consequences of the present work. Firstly, we have presented a simple relation predicting the sign of the Stokes V area asymmetry produced by gradients in velocity and magnetic inclination. From this sign it is straightforward to obtain the sign of the BBC.

Secondly, we have demonstrated that it is possible to reproduce BBC observations without having to introduce a global change of the field strength, vertical magnetic inclination or the magnetic azimuthal angle in the sunspot. In our model a considerable BBC is produced even if the magnetic inclination, field strength, and azimuth at the bottom of the atmosphere are the same as at its top. This property removes the main obstacle faced by the $\Delta\gamma$ mechanism proposed by Sánchez Almeida & Lites (cf. Solanki et al. 1993a). Consequently, the observed BBC does not necessitate a flattening of the field lines with depth, in contrast to the conclusion drawn by Sánchez Almeida & Lites (1992). They invoked this particular geometry of the field in order to be consistent with the often quoted increase of the Evershed velocity with depth (e.g. St John 1913; Schröter et al. 1989).

We see two straightforward minor extensions of our model which make it qualitatively consistent with the observed change in the Evershed line shifts and asymmetries with line strength. The first possibility is to superpose a smooth vertical velocity gradient onto the velocity field of the model used so far. An example of such a modified velocity structure is to have v_1 and v_2 values which decrease smoothly with height. The very rapid changes in $v_{\rm LOS}$ at the boundary of the horizontal flux tube remain, so that the BBC signature of the model should not be significantly affected (the rapid change in $v_{\rm LOS}$ at the interfaces is vastly more efficient in producing a BBC than the gradual change in $v_{\rm LOS}$; Solanki 1989).

Another way of reproducing observations of the Evershed effect with a model such as ours has been pointed out by Degenhardt (1993). He showed that the very extensive data of Ichimoto

(1987) can be reproduced even by a velocity that *increases* with height, if the "filling factor" of the flowing material decreases with height. For our model this means that neither v_1 nor v_2 need vary with height in order to reproduce the Evershed observations. It is sufficient if the number density of horizontal flux tubes decreases with height. The expected observational signature of such a distribution depends on the size of the spatial resolution element relative to the width of the individual flux tubes. If the flux tubes are spatially unresolved, then the proposed decrease in number density with height should lead to the line shifts and asymmetries measured at relatively low spatial resolution (cf. Degenhardt 1993). If the flux tubes are resolved, then the line shifts and asymmetries should depend strongly on spatial position. High spatial resolution line profile observations show different (Stokes I) asymmetries in bright and dark filaments and from one bright, or dark, filament to another (Wiehr et al. 1984). This may constitute support for the proposal that the number density of horizontal flux tubes decreases with height. It also suggests that these observations are beginning to resolve the flux tubes, i.e., they do not average over many of them, but further observations and modelling are required to decide these points.

The third consequence: The presence of vertical magnetic interfaces in the penumbral photosphere. One major difference between high resolution images and BBC observations is that while the former provide information on the horizontal geometry of the field, the latter contains information on its vertical structure. It is easy to see that without a vertical stratification the observed BBC cannot be reproduced, even if horizontally neighbouring filaments have highly different inclinations (e.g. no BBC would be produced at azimuths 0 and 180°, just where the observed BBC is largest). Thus the very presence (and the strength) of the observed BBC implies the existence of strong *vertical* inhomogeneities in the magnetic vector. By combining the results of high-resolution and BBC observations we, therefore, begin to obtain a rudimentary empirical picture of the 3-D structure of the fine-scale magnetic field in the photospheric layer of sunspot penumbrae.

The magnetic field is composed of two components. The more horizontal component of the field is filamented into structures with a horizontal width of at the most a few hundred km — it corresponds roughly to the width of the white-light penumbral filaments (e.g. Title et al. 1992) — and a vertical diameter which we expect to be greater than 30–50 km, a limit set by the fact that a single tube thinner than 30–50 km does not give a sufficiently large BBC signal to reproduce the observations. This limit must be considered weak, since it may be possible to enhance the BBC by placing many thin flux tubes below each other at the correct separation. The following argument suggests a rough upper limit on the vertical diameter of the flux tubes. At least one (upper or lower) boundary of the horizontal filament must lie within the formation height range of medium-strong lines over more than roughly 30% of the penumbral surface in order to reproduce the observed magnitude of the BBC for reasonable $\Delta\gamma$ and v. Unless there is a physical mechanism which ensures that one boundary lies within this relatively narrow range, this condition will be fulfilled only if the filaments are not much broader than the height-range of line formation, i.e. 200–300 km and if the vertical distance between two neighbouring filaments is of a similar order. The more vertical component of the field, according to this picture, threads its way around the horizontal filaments, as illustrated in Fig. 1. In many ways the magnetic structure proposed here is similar to the fallen magnetic flux tube model of Wentzel (1992) and our horizontal FTs may well correspond to fallen tubes. Note, however, that neither the physical processes leading to the formation of fallen tubes nor their detailed structure enter into our model. Its success supports, but by no means proves the existence of fallen flux tubes.

Fourthly, the presence of two magnetic components with the outlined structure implies a local variation of the field strength with height. At a height at which horizontal filaments lie relatively close together, the field strength is higher (in both components) than at a height at which only a relatively inclined field is present (purely due to geometrical and flux conservation arguments). At present it is unclear whether this small-scale fluctuation of B is responsible for the excess σ-component widths of the 12 μm emission lines in the penumbra (Deming et al. 1988; Hewagama et al. 1993; cf. Wentzel 1992), but it may explain why vertical field strength gradients determined by comparing B measured in two spectral lines with different formation heights are much larger than gradients derived from vector magnetograms using $\mathrm{div}\,\mathbf{B} = 0$ (e.g. Hagyard et al. 1983; Hofmann & Rendtel 1989). When applying the latter technique always a single magnetic component has been assumed. In a more realistic and complex 2-component structure, larger vertical gradients of B are compatible with relatively homogeneous transverse fields (at the low spatial resolution of the observations) and $\mathrm{div}\,\mathbf{B} = 0$.

Fifthly, the present analysis supports observations suggesting that the Evershed flow is more horizontal than the magnetic field (e.g. Maltby 1964; Title et al. 1992). Within the constraints of our simple model we find that the velocity in the more horizontal magnetic filaments is 1.5–1.7 times larger than in the more vertical component. Not the exact numerical value of the velocity ratio is important, since we expect it to be changed considerably by a more detailed model, but rather the fact that the velocity *is* larger in the horizontal magnetic component. The BBC thus provides a spatial-resolution independent, if model-affected, means of determining the velocity ratio in the two components. The fact that the velocity is more horizontal than the magnetic field also provides an, at least qualitatively correct, explanation for the observation that the velocity neutral line in general lies on the centre-side of the magnetic neutral line (see Pevtsov 1992 and references therein).

Note that although we have, for simplicity, assumed the Evershed effect to be due to a mass flow, another mechanism for producing net line shifts, e.g. waves (Maltby & Eriksen 1967; Darconza 1992; Bünte et al. 1993), should, in principle, also result in a BBC of similar magnitude.

In spite of the surprising success of the proposed simple model, we cannot as yet rule out other geometries (e.g. in-

clined flux tubes embedded in a relatively horizontal field, or intertwined flux tubes with different inclinations). Nevertheless, we are confident that further investigations of the BBC will yield additional constraints on the structure of sunspot magnetic fields. We feel that the most important steps needed to realize the potential of the BBC as a diagnostic are improved observations of the BBC and the introduction of more realism into the model. Higher spatial-resolution observations and correlations with other magnetic or thermodynamic parameters, e.g. γ', B, temperature, would be useful. An improvement in our knowledge of the exact small-scale variation of γ', B, v and continuum intensity would also be of great advantage. Future investigations should incorporate the information obtained from quantitative analyses of the difference in position of velocity and magnetic neutral lines. Proposed improvements to the model include calculating the V profiles along numerous rays passing through the horizontal flux tube, taking into account the small-scale variation of the azimuthal angle of the field, as well as considering lines-of-sight for which the net azimuth of the field is not zero. Finally, the dependence of the NCP on line parameters like equivalent width and Landé factor also need to be investigated.

References

Abdussamatov, H.I., Krat, V.A., 1970, Sol. Phys. 14, 132
Auer, L.H., Heasley, J.N., 1978, A&A 64, 67
Babcock H.W., 1951, ApJ 114, 1
Beckers, J.M., Schröter, E.H., 1969, Sol. Phys. 10, 384
Bünte M., Darconza G., Solanki S.K., 1993, A&A in press
Darconza G., 1992, Diplomarbeit, ETH Zürich
Degenhardt D., 1993, A&A submitted
Degenhardt D., Wiehr E., 1991, A&A 252, 821
Deming, D., Boyle, R.J., Jennings, D.E., Wiedemann, G., 1988, ApJ 333, 978
Deuber F.-L., Fleck B., Hofmann J., Schmidt W., 1993, in The Magnetic and Velocity Fields of Solar Active Regions, H. Zirin (Ed.), Astron. Soc. Pacific Conf. Ser., in press.
Golovko A.A., 1974, Sol. Phys. 37, 113
Grigorjev V.M., Katz J.M., 1972, Sol. Phys. 22, 119
Grigorjev, V.M., Katz, J.M., 1975, Sol. Phys. 42, 21
Grossmann-Doerth, U., Schüssler, M., Solanki, S.K., 1988, A&A 206, L37
Grossmann-Doerth, U., Schüssler, M., Solanki, S.K., 1989, A&A 221, 338
Hagyard M.J., Teuber D., West E.A., Tandberg-Hanssen E., Henze W., Beckers J.M., Bruner M., Hyder C.L., Woodgate B.E., 1983, Sol. Phys. 84, 13
Henson G.D., Kemp J.C., 1984, Sol. Phys. 93, 289
Hewagama T., Deming D., Jennings D.E., Osherovich V., Wiedemann G., Zipoy D., Mickey D.L., Garcia H., 1993, ApJ in press
Hofmann, A., Rendtel, J., 1989, Astron. Nachr. 310, 61
Ichimoto, K., 1987, PASJ 39, 329
Illing, R.M.E., 1981, ApJ 248, 358
Illing, R.M.E., Landman, D.A., Mickey, D.L., 1974a, A&A 35, 327
Illing, R.M.E., Landman, D.A., Mickey, D.L., 1974b, A&A 37, 97
Illing, R.M.E., Landman, D.A., Mickey, D.L., 1975, A&A 41, 183
Kemp, J.C., Henson, G.D., 1983, ApJ 266, L69
Landman, D.A., Finn, G.D., 1979, Sol. Phys. 63, 221
Lites B.W., Elmore D.F., Tomczyk S., Seagraves P., Skumanich A., Streander K.V., 1993, in The Magnetic and Velocity Fields of Solar Active Regions, H. Zirin (Ed.), Astron. Soc. Pacific Conf. Ser., in press.
Makita, M., 1981, in *Proc. Japan–France Seminar on Solar Physics*, F. Moriyama and J.C. Henoux (Eds.), University of Tokyo Press, Tokyo, p. 99
Makita, M., 1986, Sol. Phys. 106, 269
Makita M., Ohki Y., 1986, Ann. Tokyo Astron. Obs. 21, 1
Maltby P., 1964, *Astrophys. Novegica* **8**, 205
Maltby P., Eriksen G., 1967, Sol. Phys. 2, 249
Maltby, P., Avrett, E.H., Carlsson, M., Kjeldseth-Moe, O., Kurucz, R.L., Loeser, R., 1986, ApJ 306, 284
Mamadazimov, M., 1972, Sol. Phys. 22, 129
Mickey D.L., 1985a, in Measurements of Solar Vector Magnetic Fields, M.J. Hagyard (Ed.), NASA Conference Publ., CP-2374, p. 183
Mickey D.L., 1985b, Sol. Phys. 97, 223
Montavon C., 1992, Diplomarbeit, ETH Zürich
Moore, C.E., 1972, *A Multiplet Table of Astrophysical Interest*, National Bureau of Standards, Washington, D.C., NSRDS–NBS 40.
Murphy, G.A., 1990, NCAR Cooperative Thesis No. 124
Mürset, U., Solanki, S.K., Stenflo, J.O., 1988, A&A 204, 279
Parker E.N., 1992, in Sunspots: Theory and Observations, J.H. Thomas, N.O. Weiss (Eds.), Kluwer, Dordrecht, p. 413
Pevtsov A.A., 1992, Sol. Phys. 141, 65
Rees, D.E., Murphy, G.A., Durrant, C.J., 1989, ApJ 339, 1093
Sánchez Almeida, J., Collados, M., Del Toro Iniesta, J.C., 1988, A&A 201, L37
Sánchez Almeida, J., Collados, M., Del Toro Iniesta, J.C., 1989, A&A 222, 311
Sánchez Almeida J., Lites B.W., 1992, ApJ 398, 359
Schmidt W., Hofmann A., Balthasar H., Tarbell T.D., Frank Z.A., 1992, A&A 264, L27
Schröter E.H., 1965, *Z. Astrophys.* **62**, 256.
Schröter E.H., Kentischer T., Münzer H., 1989, in High Spatial Resolution Solar Observations, O. von der Lühe (Ed.), National Solar Obs., Sunspot, NM, p. 299
Skumanich, A., Lites, B.W., 1987, ApJ 322, 483
Skumanich, A., Lites, B.W., 1991, in Solar Polarimetry, L. November (Ed.), National Solar Observatory, Sunspot, NM, p. 307
Solanki, S.K., 1989, A&A 224, 225
Solanki, S.K., Pahlke, K.D., 1988, A&A 201, 143
Solanki S.K., Schmidt H.U., 1993, A&A 267, 287.
Solanki S.K., Rüedi I., Livingston W., 1992, A&A 263, 339
Solanki S.K., Walther U., Livingston W., 1993a, A&A submitted.
Solanki S.K., Montavon C.A.P., Livingston W., 1993b, A&A submitted.
St. John C.E., 1913, ApJ 37, 322
Stellmacher G., Wiehr E., 1971, Sol. Phys. 17, 21
Stellmacher G., Wiehr E., 1980, A&A 82, 157
Thévenin F., 1990, A&AS 82. 179
Title A.M., Frank Z.A., Shine R.A., Tarbell T.D., Topka K.P., Scharmer G., Schmidt W., 1992, in Sunspots: Theory and Observations, J.H. Thomas, N.O. Weiss (Eds.), Kluwer, Dordrecht, p. 195
Wentzel D.G., 1992, ApJ 388, 211
Wiehr E., Koch A., Knölker M., Küveler G., Stellmacher G., 1984 , A&A 140, 352